JJMIE

Volume 12, Number 3, October. 2018
ISSN 1995-6665
Pages 215 - 229

Jordan Journal of Mechanical and Industrial Engineering

Exact Thermomechanical Characteristics of a Pressurized Rotating Circular Annulus or a Disc Made of Functionally Graded (FG) Hypothetical and Physical Materials

Vebil Yıldırım

Department of Mechanical Engineering, University of Çukurova, Adana, Turkey

Received 3 Jun. 2018

Abstract

In the present study, thermomechanical characteristics of a functionally graded (FG) uniform traction-free circular annulus are determined analytically under separate and combined centrifugal, steady-state thermal and pressure loads based on the one-dimensional axisymmetric plane-stress assumption. It is assumed that elasticity modulus, density, thermal expansion coefficient and thermal conductivity are all to be continuously changed in the radial direction with different inhomogeneity indexes of a simple power law material grading rule while Poisson's ratio is kept constant. Hypothetically and physically chosen metal-ceramic pairs such as nickel-silicon nitride (Ni-Si_3N_4), aluminum-aluminum oxide (Al-Al_2O_3), and stainless steel-zirconium oxide ($SUS304$-ZrO_2) are included in the parametric studies. Results of conducting separate and combined effects of centrifugal, thermal, and pressure loadings are presented in both tabular and graphical forms in a comparative manner. Those works mostly suggest that the effect of thermal loads may be either negligible compared to inertia forces or may be having higher importance than the inertias. It is also deduced that the thermal characteristics of both individual metal and ceramic are totally different from FGM's thermal traits.

Keywords: Thermomechanical, exact solution, functionally graded, circular annulus, rotating disc;

1. Introduction

As commonly known, functionally graded materials (FGM) have exceptional gradually changing mechanical and thermal properties along the preferred directions of the structure [1-2]. Due to this reason, they have gained great attention from many investigators. The significant number of studies have focused on the investigation of the elastic behavior of rotating circular annulus or discs which may be subject to individual or combined effects of mechanical and thermal loads. Investigations related to only a uniform circular annulus or a disc are to be considered in the following literature survey and have been classified by the load types as well.

Under only centrifugal force: By employing a simple-power rule, Horgan and Chan [3] analytically investigated the effects of material inhomogeneity on the response of linearly elastic isotropic solid circular disks or cylinders, rotating at a constant angular velocity about a central axis. Durodola and Attia [4] studied deformation and stressed the FG rotating disks by a direct numerical integration of the governing differential equations as well as the finite element method. Zenkour [5] presented an elastic solution in terms of Whittaker's functions for exponentially graded uniform rotating annular disks. He considered combinations of clamped and free boundary conditions. Zenkour [6] later considered a rotating functionally graded annular disk with rigid casing. Eraslan and Akış [7] used two variants of a parabolic profile function for disks made of functionally graded materials. Generalizing an available two-dimensional plane-stress solution to a three-dimensional one, Asghari and Ghafoori [8] proposed a semi-analytical three-dimensional elasticity solution for rotating FG hollow and solid disks. Under the assumptions of plane stress, isotropy, and small deformations, Argeso [9] considered analytically both a homogeneous non-uniform rotating disk, and a FG uniform disc. He verified the results by the nonlinear shooting method. Peng and Li [10] employed Fredholm integrals for elastic analysis of arbitrarily graded uniform solid rotating disks. By employing the elasto-perfectly-plastic material model based on Tresca's yield criterion, Nejad et al. [11] presented firstly exact solutions for elasto-plastic deformations and stresses in a simple-power law graded rotating disk. Their work revealed that the plasticity can occur in different regions of the disk. By utilizing Runge-Kutta and shooting methods, Dai and Dai [12] considered the variation of angular speed of a FGM uniform rotating disc. Çallıoğlu et al. [13] investigated elastic–plastic stress analysis with non-work hardening case of power-law graded discs subjected to a constant angular velocity. They verified the results by Ansys.

* Corresponding author e-mail: vebil@cu.edu.tr.

Under only pressure loads: Horgan and Chan [14] showed that the stress response of an inhomogeneous cylinder (or disk) subjected to pressure is significantly different from that of a homogeneous body. Based on the hypergeometric functions, You et al. [15] presented an analytical solution for circular linearly graded uniform disks subject to internal and/or external pressure. Tutuncu and Temel [16] studied axisymmetric displacements and stresses in FG hollow cylinders, disks and spheres subject to only uniform internal pressure by using plane elasticity theory and complementary functions method. Lotfian et al. [17] presented a two-dimensional elasticity solution and a numerical solution using finite element method for elastic analysis of parabolically graded uniform disk subjected to both the internal and external pressures. Nejad et al. [18] extended the previous study by Lotfian et al. [17] to exponentially graded uniform discs that were subjected to internal and external pressures.

Under only thermal loads: Noda [19] has reviewed works conducted in 1980-1991 which covers a wide range of topics from thermo-elastic to thermo-inelastic problems with temperature-dependent properties. Tanigawa [20] also presented a comprehensive review on thermoelastic analysis of FGMs. Bakshi et al. [21] worked on coupled thermoelasticity of functionally graded disks. Tokovy and Ma [22] studied thermal stresses in anisotropic and radially inhomogeneous annular domains. Zenkour [23] carried out a functionally graded annular sandwich disk subjected to only steady-state thermal load. He presented a closed form solution in terms of Whittaker's functions. Peng and Li [24] studied analytically and numerically thermoelastic analysis of either power-law graded annulus or arbitrarily graded annulus. They transformed the governing equation to a Fredholm integral equation. Based on the two-dimensional thermoelastic theories and finite difference method, Arnab et al. [25] investigated numerically thermoelastic fields in a thin circular power-law and exponentially graded Al_2O_3/Al disk with a concentric hole subjected to thermal loads. Under a logarithmic thermal gradients assumption, Aleksandrova [26] investigated analytically elasto-plastic thermal stresses and deformations in a thin annular plate embedded into a rigid container and made of a homogeneous and isotropic material based on the von Mises yield criterion with its associated flow rule.

Under combined pressure and thermal loads: Çallıoğlu et al. [27] analytically studied thermoelastic analysis of power-law graded stress-free annular discs subjected to both pressure and various assumed temperature distributions. Kurşun et al. [28] worked on the elastic stress analysis of power-law graded annular discs subjected to both uniform pressures on the inner surface and a linearly decreasing temperature distribution. Gönczi and Ecsedi [29] solved analytically and numerically governing equation govern the thermo-mechanical behavior of a hollow power-law graded stress-free uniform circular disc under axisymmetric pressure and thermal loads.

Under combined magnetic and thermal loads: Combined effects of magnetic and thermal loads on the elastic behavior of exponentially graded uniform annular discs were considered by Zenkour [30].

Under combined centrifugal and thermal loads: Zenkour [31] also proposed an analytical solution in terms of Whittaker's functions for exponentially graded uniform rotating annular disks under steady-state thermal and centrifugal loads. By dividing the radial domain into some virtual sub-domains, Kordkheili and Naghdabadi [32] presented a semi-analytical solution for a thin axisymmetric uniform rotating traction-free disk made of functionally graded materials with power-law distribution of the volume fraction under centrifugal force and uniform thermal loadings. Go et al. [33] developed a finite element method to demonstrate that a circular power-law graded free-free uniform cutter or grinding disk can be designed with better thermo-elastic characteristics if certain parameters, namely, temperature distribution, angular speed, radial thickness, and outer surface temperature, are controlled properly. A finite element model was developed by Afsar et al. [34] using the variational approach and Ritz method to study the thermoelastic characteristics due to a thermal load and rotation of a thin uniform circular rotating disk having a concentric hole and an exponentially-graded coating at the outer surface. Based on the two-dimensional thermoelastic theories, Afsar and Go [35] conducted a finite element analysis of thermoelastic field in a thin circular exponentially graded Al_2O_3/Al disk subjected to a thermal load and an inertia force due to rotation of the disk. Afsar and Sohag [36] considered thermoelastic characteristics of a thin circular disc having a concentric hole and a functionally graded material (FGM) coating at the outer surface under thermal and centrifugal loads. Gong et al. [37] used a finite volume method for the steady 3-D thermoelastic analysis of the functionally graded uniform rotating discs. They showed that the least square method achieves better performances than the Gaussian method but least square method costs slightly more iteration and computer memory under different mesh types. Yıldırım [38], recently, investigated analytically the thermomechanical attributes of a power-law graded uniform mounted disc with or without rigid casing are under centrifugal and steady-state thermal loads.

In the present study, which is the complementary of Yıldırım's [38] study, a circular annulus or a disc is assumed to be made of both hypothetical and physical metal-ceramic pairs under combined pressure, centrifugal, and thermal loads (Fig. 1). A benchmark example using only hypothetical inhomogeneity indexes for both infinite FGM cylinders [39] and FGM spheres [40] is revisited with a rotating circular annulus or a disc. After this stage, another fresh study is conducted where traction-free annulus is assumed to be made of three types of physical metal-ceramic pairs. Separate and combined effects of mechanical and thermal loads are all investigated.

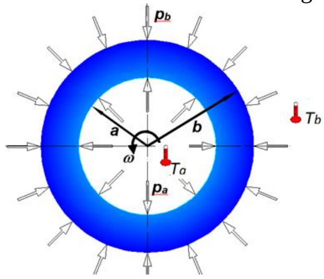

Figure 1. Combined pressure, centrifugal, and thermal loads for a traction-free annulus

2. Thermal Analysis

Let's consider a hollow disc of inside radius a, and outside radius b (Fig. 1). The radial and tangential coordinates are denoted by r, and θ. Let's use the prime symbol to indicate the derivatives with respect to the radial coordinate. For any arbitrary material grading rule of a non-uniform thermal conduction coefficient, $k(r)$, the differential equation which governs the temperature distribution along the radial coordinate in a uniform annulus/disc or a cylinder is defined by [41]

$$\frac{1}{r}\left(rk(r)T'(r)\right)' = T''(r) + T'(r)\left(\frac{1}{r}+\frac{k'(r)}{k(r)}\right) = 0 \quad (1)$$

If the following power-law grading rule

$$k(r) = k_a\left(\frac{r}{a}\right)^{\mu} \quad (2)$$

Is employed, Eq. (1) turns into the following

$$T''(r) + \frac{(1+\mu)}{r}T'(r) = 0 \quad (3)$$

Yıldırım [41] solved Eq. (3) under Dirichlet's boundary conditions, $T(a)=T_a$ and $T(b)=T_b$, as follows

$$T(r) = \frac{r^{-\mu}\left(-b^{\mu}r^{\mu}T_b + a^{\mu}\left(r^{\mu}T_a + b^{\mu}(-T_a+T_b)\right)\right)}{a^{\mu}-b^{\mu}} = \Phi_1 + r^{-\mu}\Phi_2 \quad (4)$$

where

$$\Phi_1 = \frac{a^{\mu}T_a - b^{\mu}T_b}{a^{\mu}-b^{\mu}}\ ; \quad \Phi_2 = \frac{a^{\mu}b^{\mu}(-T_a+T_b)}{a^{\mu}-b^{\mu}} \quad (5)$$

Solution of Eq. (3) for isotropic and homogeneous materials, $=0$, under the same boundary conditions takes the following form [41]

$$T(r) = T_a + \frac{(T_b-T_a)}{ln(\frac{b}{a})}l\,n\left(\frac{r}{a}\right) = lnr\Psi_2 + \Psi_1$$
$$\Psi_1 = \frac{lnaT_b - T_a lnb}{ln(\frac{a}{b})}\ ; \quad \Psi_2 = \frac{T_a - T_b}{ln(\frac{a}{b})} \quad (6)$$

3. Derivation of Governing Equation

Under axisymmetric plane-stress assumptions, the strain-displacement relations for cylinders are given by

$$\epsilon_r(r) = u_r'(r);\ \epsilon_\theta(r) = \frac{u_r(r)}{r} \quad (7)$$

where u_r is the radial displacement, ε_r is the unit radial strain, ε_θ is the unit tangential strain. Thermoelastic stress–strain constitutive relations for a FGM may be given in the form of [38]

$$\sigma_r(r) = C_{11}(r)\epsilon_r + C_{12}(r)\epsilon_\theta - \left(C_{11}(r)+C_{12}(r)\right)\alpha(r)T(r)$$
$$\sigma_\theta(r) = C_{12}(r)\epsilon_r + C_{11}(r)\epsilon_\theta - \left(C_{11}(r)+C_{12}(r)\right)\alpha(r)T(r) \quad (8)$$

where $\sigma_r(r)$ is the radial stress, $\sigma_\theta(r)$ is the hoop stress, $\alpha(r)$ is the coefficient of thermal expansion, and

$$C_{11}(r) = \frac{1}{1-\nu^2}E(r)\ ;\ C_{12}(r) = \frac{\nu}{1-\nu^2}E(r) = \nu C_{11}(r) \quad (9)$$

where $E(r)$ is Young's modulus and ν is Poisson's ratio. The arithmetic mean of Poisson's ratios of ceramic and metal is used in the present numerical calculations. Substituting Eq. (7) into Eq. (8), Hooke's law, then, takes the following form of

$$\sigma_r(r) = C_{11}(r)\left(u_r'(r) + \nu\frac{u_r(r)}{r}\right) - (1+\nu)C_{11}(r)\alpha(r)T(r)$$
$$\sigma_\theta(r) = C_{11}(r)\left(\nu\, u_r'(r) + \frac{u_r(r)}{r}\right) - (1+\nu)C_{11}(r)\alpha(r)T(r) \quad (10)$$

The equilibrium equation in the radial coordinate of an annulus/disc rotating at a constant circular velocity, ω, is

$$\left(r\sigma_r(r)\right)' - \sigma_\theta = \sigma_r'(r) + \frac{\sigma_r(r)-\sigma_\theta(r)}{r} = -\rho(r)\omega^2 r \quad (11)$$

where $\rho(r)$ is the material density. After substitution of Eq. (10) into Eq. (11), Navier equation in general form is obtained.

$$u_r''(r) + \left(\frac{1}{r}+\frac{C_{11}'(r)}{C_{11}(r)}\right)u_r'(r) + \left(-\frac{1}{r^2}+\frac{\nu}{r}\frac{C_{11}'(r)}{C_{11}(r)}\right)u_r(r) = -\frac{\rho(r)\omega^2 r}{C_{11}(r)} + (1+\nu)\alpha(r)T'(r) + \left(\frac{C_{11}'(r)}{C_{11}(r)}\alpha(r) + \alpha'(r)\right)(1+\nu)T(r) \quad (12)$$

If the following material gradients are used in Eq. (12),

$$E(r) = E_a\left(\frac{r}{a}\right)^{\beta};\quad \rho(r) = \rho_a\left(\frac{r}{a}\right)^{q};\quad \alpha(r) = \alpha_a\left(\frac{r}{a}\right)^{n} \quad (13)$$

then Navier equation for thermomechanical analysis of a power-law graded annulus/disc is obtained as follows [38]

$$\frac{(-1+\beta\nu)}{r^2}u_r(r) + \frac{(1+\beta)}{r}u_r'(r) + u_r''(r) = -\frac{a^{-q+\beta}r^{1+q-\beta}(1-\nu^2)\rho_a\omega^2}{E_a} + a^{-n}r^{-1+n-\mu}\alpha_a(1+\nu)\left(r^{\mu}(n+\beta)\Phi_1 + (n+\beta-\mu)\Phi_2\right) \quad (14)$$

where inhomogeneity indexes are denoted by β, q, μ and $, n$. By using the followings,

$$\Delta_1 = a^{-n}\alpha_a(n+\beta)(1+\nu)\Phi_1$$
$$\Delta_2 = a^{-n}\alpha_a(n+\beta-\mu)(1+\nu)\Phi_2 \quad (15)$$

Navier equation may be rewritten in a more compact form as

$$\frac{(-1+\beta\nu)}{r^2}u_r(r) + \frac{(1+\beta)}{r}u_r'(r) + u_r''(r) = -\frac{a^{-q+\beta}r^{1+q-\beta}(1-\nu^2)\rho_a\omega^2}{E_a} + r^{-1+n-\mu}\left(r^{\mu}\Delta_1 + \Delta_2\right) \quad (16)$$

This is a second order non-homogeneous Euler-Cauchy differential equation with constant coefficients [38]. It is possible to find a closed form general solution (homogeneous+particular) to this equation. After getting the solution, combined radial and hoop stresses may be determined based on the superposition principle for linearly elastic materials as follows.

$$\sigma_{total} = \sigma_{thermal} + \sigma_{rotation} + \sigma_{pressure} \quad (17)$$

Equivalent stress at any surface in the radial direction is computed with the help of von-Mises failure criterion as follows

$$\sigma_{eq}(r) = \sqrt{\sigma_r^2 - \sigma_r\sigma_\theta + \sigma_\theta^2} \tag{18}$$

The general solutions of Eq. (16), obtained with the help of Euler-Cauchy technique, are given directly in the following sections for each separate mechanical and thermal load.

3.1. Elastic Fields under both Internal and External Pressures

Homogeneous solution of the Navier equation in Eq. (16)

$$\frac{(-1+\beta\nu)}{r^2}u_r(r) + \frac{(1+\beta)}{r}u_r'(r) + u_r''(r)=0 \tag{19}$$

under boundary conditions, $\sigma_r(a) = -p_a$ and $\sigma_r(b) = -p_b$, renders the elastic field due to both internal and external pressures, p_a and p_b, as follows

Explicit forms of Eq. (20) are as follows

$$u_r(r) = r^{\frac{1}{2}(-\beta-\xi)}\left(A_1 + A_2 r^\xi\right)$$

$$\sigma_r(r) = -\frac{1}{2}C_{11}(r)r^{\frac{1}{2}(-2-\beta-\xi)}\left(A_2 r^\xi(\beta - 2\nu - \xi) + A_1(\beta - 2\nu + \xi)\right) \tag{20}$$

$$\sigma_\theta(r) = \frac{1}{2}r^{\frac{1}{2}(-2-\beta-\xi)}C_{11}(r)\left(A_2 r^\xi(2 - \beta\nu + \nu\xi) - A_1\left(-2 + \nu(\beta+\xi)\right)\right)$$

Where

$$\xi = \sqrt{4 + \beta^2 - 4\beta\nu} \tag{21a}$$

$$A_1 = -\frac{2(\nu^2-1)a^{\frac{\beta+\xi}{2}}b^{\frac{\xi-\beta}{2}}\left(bp_b a^{\frac{\beta+\xi}{2}} - ap_a b^{\frac{\beta+\xi}{2}}\right)}{E_a(a^\xi - b^\xi)(\beta - 2\nu + \xi)} \tag{21b}$$

$$A_2 = \frac{b^{-\beta/2}\left(2(\nu^2-1)p_b a^\beta b^{\frac{\xi}{2}+1} - 2(\nu^2-1)p_a b^{\beta/2}a^{\frac{1}{2}(\beta+\xi+2)}\right)}{E_a(a^\xi - b^\xi)(\beta - 2\nu - \xi)} \tag{21c}$$

$$u_r(r) = \frac{2(\nu^2-1)p_a a^{\frac{1}{2}(\beta+\xi+2)}r^{\frac{1}{2}(-\beta-\xi)}\left(b^\xi(\beta-2\nu-\xi) - r^\xi(\beta-2\nu+\xi)\right)}{E_a(a^\xi-b^\xi)(\beta-2\nu-\xi)(\beta-2\nu+\xi)} + \frac{2(\nu^2-1)p_b a^\beta b^{\frac{1}{2}(-\beta+\xi+2)}r^{\frac{1}{2}(-\beta-\xi)}\left(a^\xi(\beta-2\nu-\xi) - r^\xi(\beta-2\nu+\xi)\right)}{E_a(a^\xi-b^\xi)(\beta-2\nu+\xi)(-\beta+2\nu+\xi)} \tag{22a}$$

$$\sigma_r(r) = \frac{p_a a^{\frac{1}{2}(-\beta+\xi+2)}(b^\xi - r^\xi)r^{\frac{1}{2}(\beta-\xi-2)}}{a^\xi - b^\xi} + \frac{p_b(a^\xi - r^\xi)b^{\frac{1}{2}(-\beta+\xi+2)}r^{\frac{1}{2}(\beta-\xi-2)}}{b^\xi - a^\xi} \tag{22b}$$

$$\begin{aligned}\sigma_\theta(r) = {} & \frac{1}{(a^\xi-b^\xi)(\beta-2\nu-\xi)(\beta-2\nu+\xi)}\Big(p_a a^{\frac{1}{2}(-\beta+\xi+2)}r^{\frac{1}{2}(\beta-\xi-2)}\big(b^\xi(\beta-2\nu-\xi)(\nu(\beta+\xi)-2) \\ & + r^\xi(\beta-2\nu+\xi)(-\beta\nu+\nu\xi+2)\big)\Big) \\ & + \frac{1}{(a^\xi-b^\xi)(\beta-2\nu+\xi)(-\beta+2\nu+\xi)}\Big(p_b b^{\frac{1}{2}(-\beta+\xi+2)}r^{\frac{1}{2}(\beta-\xi-2)}\big(a^\xi(\beta-2\nu-\xi)(\nu(\beta \\ & +\xi)-2) + r^\xi(\beta-2\nu+\xi)(-\beta\nu+\nu\xi+2)\big)\Big)\end{aligned} \tag{22c}$$

For a disk made of an isotropic and homogeneous material, solution of the following under boundary conditions, $\sigma_r(a) = -p_a$ and $\sigma_r(b) = -p_b$,

$$u_r''(r) + \frac{1}{r}u_r'(r) - \frac{1}{r^2}u_r(r) = 0 \tag{23}$$

gives the elastic field due to both internal and external pressures as follows [42]

$$u_r(r) = -\frac{a^2p_a(b^2(\nu+1) - (\nu-1)r^2)}{Er(a^2-b^2)} + \frac{b^2p_b(a^2(\nu+1) - (\nu-1)r^2)}{Er(a^2-b^2)}$$

$$\sigma_r(r) = \frac{a^2p_a(b^2-r^2)}{r^2(a^2-b^2)} + \frac{b^2(a-r)(a+r)p_b}{r^2(b^2-a^2)} \tag{24}$$

$$\sigma_\theta(r) = -\frac{a^2p_a(b^2+r^2)}{r^2(a^2-b^2)} + \frac{b^2(a^2+r^2)p_b}{r^2(a^2-b^2)}$$

3.2. Elastic Fields under Rotation at a Constant Angular Speed

Homogeneous and particular solutions of the Navier equation given in Eq. (16)

$$\frac{(-1+\beta\nu)}{r^2}u_r(r)+\frac{(1+\beta)}{r}u_r'(r)+u_r''(r)= -\frac{a^{-q+\beta}r^{1+q-\beta}(1-\nu^2)\rho_a\omega^2}{E_a} \quad (25)$$

give the elastic fields in terms of integration constants due to the rotation about an axis passing through the center of annulus as

$$u_r(r)=r^{-\beta}\left(r^{\frac{\beta-\xi}{2}}\left(B_1+B_2r^{\xi}\right)+r^{3+q}\Omega\right)$$

$$\sigma_r(r)=\frac{1}{2}r^{-1-\beta-\frac{\xi}{2}}C_{11}(r)\left(r^{\beta/2}\left(-B_1(\beta-2\nu+\xi)+B_2r^{\xi}(-\beta+2\nu+\xi)\right)+2r^{3+q+\frac{\xi}{2}}(3+q-\beta+\nu)\Omega\right) \quad (26)$$

$$\sigma_\theta(r)=\frac{1}{2}r^{-1-\beta-\frac{\xi}{2}}C_{11}(r)\left(-r^{\beta/2}\left(-B_2r^{\xi}(2-\beta\nu+\nu\xi)+B_1\left(-2+\nu(\beta+\xi)\right)\right)+2r^{3+q+\frac{\xi}{2}}(1+(3+q-\beta)\nu)\Omega\right)$$

where

$$\xi=\sqrt{4+\beta^2-4\beta\nu}$$

$$\Omega=\frac{a^{-q+\beta}(-1+\nu^2)\rho_a\omega^2}{E_a(8+q(6+q-\beta)-3\beta+\beta\nu)} \quad (27)$$

Integration constants in Eq. (26) are determined under free-free boundary conditions, $\sigma_r(a)=0$ and $\sigma_r(b)=0$, as

$$B_1=\frac{2\Omega a^{\frac{\xi-\beta}{2}}b^{\frac{\xi-\beta}{2}}(\beta-\nu-q-3)\left(a^{q+3}b^{\frac{\beta+\xi}{2}}-b^{q+3}a^{\frac{\beta+\xi}{2}}\right)}{(a^{\xi}-b^{\xi})(\beta-2\nu+\xi)}$$

$$B_2=\frac{2\Omega a^{-\beta/2}b^{-\beta/2}(-\beta+\nu+q+3)\left(b^{\beta/2}a^{\frac{\xi}{2}+q+3}-a^{\beta/2}b^{\frac{\xi}{2}+q+3}\right)}{(a^{\xi}-b^{\xi})(\beta-2\nu-\xi)} \quad (28)$$

If the disk material is homogeneous and isotropic, then, Eq. (25) turns into the following

$$u_r''(r)+\frac{1}{r}u_r'(r)-\frac{1}{r^2}u_r(r)=-\frac{\rho\omega^2r}{C_{11}}=-\frac{r(1-\nu^2)\rho\omega^2}{E} \quad (29)$$

Solution of this equation given above under the free-free boundary conditions is [43]

$$u_r(r)=\frac{1}{8Er}\left(\rho\omega^2\left(a^2(\nu+3)(b^2(\nu+1)-(\nu-1)r^2)-(\nu-1)r^2(b^2(\nu+3)-(\nu+1)r^2)\right)\right)$$

$$\sigma_r(r)=\frac{(\nu+3)\rho\omega^2(a-r)(a+r)(r^2-b^2)}{8r^2} \quad (30)$$

$$\sigma_\theta(r)=\frac{\rho\omega^2\left(a^2(\nu+3)(b^2+r^2)+r^2(b^2(\nu+3)-(3\nu+1)r^2)\right)}{8r^2}$$

3.3. Elastic Fields under Thermal Loads

Homogeneous and particular solutions of Navier equation given in Eq. (16) together with Dirichlet's boundary conditions, $T(a)=T_a$ and $T(b)=T_b$,

$$\frac{(-1+\beta\nu)}{r^2}u_r(r)+\frac{(1+\beta)}{r}u_r'(r)+u_r''(r)=r^{-1+n-\mu}(r^{\mu}\Delta_1+\Delta_2) \quad (31)$$

give the elastic field as

$$u_r(r)=\Delta_3\left(r^{1+n-\mu}\Delta_4+r^{1+n}\Delta_1\Delta_5+C_1r^{\frac{1}{2}(-\beta-\xi)}\Delta_5\Delta_6+C_2r^{\frac{1}{2}(-\beta+\xi)}\Delta_5\Delta_6\right)$$

$$\begin{aligned}\sigma_r(r)&=C_{11}(r)r^n\Delta_3\left(\Delta_1\Delta_5(1+n+\nu)+r^{-\mu}\Delta_4(1+n-\mu+\nu)\right)\\&+\frac{1}{2}C_{11}(r)r^{\frac{1}{2}(-2-\beta-\xi)}\Delta_3\Delta_5\Delta_6\left(-C_1(\beta-2\nu+\xi)+C_2r^{\xi}(-\beta+2\nu+\xi)\right)\\&+\frac{a^{-n-\beta}E_ar^{n+\beta-\mu}\alpha_a(r^{\mu}\Phi_1+\Phi_2)}{-1+\nu}\end{aligned}$$

$$\begin{aligned}\sigma_\theta(r)&=C_{11}(r)r^n\Delta_3\left(\Delta_1\Delta_5(1+\nu+n\nu)+r^{-\mu}(\Delta_4+\Delta_4(1+n-\mu)\nu)\right)\\&+\frac{1}{2}C_{11}(r)r^{\frac{1}{2}(-2-\beta-\xi)}\Delta_3\Delta_5\Delta_6\left(C_2r^{\xi}(2-\beta\nu+\nu\xi)-C_1\left(-2+\nu(\beta+\xi)\right)\right)\\&+\frac{a^{-n-\beta}E_ar^{n+\beta-\mu}\alpha_a(r^{\mu}\Phi_1+\Phi_2)}{-1+\nu}\end{aligned} \quad (32)$$

where auxiliary constants are

$$\xi=\sqrt{4+\beta^2-4\beta\nu} \quad (33a)$$

$$\Delta_3=16\left((-2-2n-\beta+\xi)(2+2n+\beta+\xi)(2+2n+\beta-2\mu+\xi)(-2-2n-\beta+2\mu+\xi)\right)^{-1} \quad (33b)$$

$$\Delta_4=\Delta_2(\beta+n(2+n+\beta)+\beta\nu)$$

$$\Delta_5=n^2+n(2+\beta-2\mu)+(-2+\mu)\mu+\beta(1-\mu+\nu)$$

$$\Delta_6=\beta+n(2+n+\beta)+\beta\nu$$

Integration constants in the solution of Eq. (32) are determined for free-free boundary conditions as

$$C_1 = \frac{2b^{\frac{1}{2}(\xi-2\mu)}a^{\frac{1}{2}(\xi-2(\mu+n))}}{\Delta_3\Delta_5\Delta_6(a^\xi - b^\xi)(\beta - 2\nu + \xi)}\Big(a^{\mu+\frac{\xi}{2}}b^{\frac{\beta}{2}+n+1}\Big(\Delta_3 a^n\big(\Delta_1\Delta_5 b^\mu(\nu+n+1) + \Delta_4(-\mu+\nu+n+1)\big) - \alpha_a(\nu+1)(\Phi_1 b^\mu + \Phi_2)\Big) + a^{\frac{\beta}{2}+n+1}b^{\mu+\frac{\xi}{2}}(-\Delta_1\Delta_3\Delta_5(\nu+n+1)a^{\mu+n} + \alpha_a(\nu+1)\Phi_1 a^\mu - \Delta_3\Delta_4 a^n(-\mu+\nu+n+1) + \alpha_a(\nu+1)\Phi_2)\Big)$$

$$C_2 = -\frac{1}{\Delta_3\Delta_5\Delta_6(a^\xi - b^\xi)(-\beta+2\nu+\xi)}2b^{-\mu}a^{-\mu-n}\Big(-\alpha_a(\nu+1)\Phi_1 b^\mu a^{\frac{\beta}{2}+\mu+n+\frac{\xi}{2}+1} - \alpha_a(\nu+1)\Phi_2 b^\mu a^{\frac{1}{2}(\beta+2n+\xi+2)} + \Delta_1\Delta_3\Delta_5 b^\mu(\nu+n+1)a^{\frac{1}{2}(\beta+2\mu+4n+\xi+2)} + \Delta_3\Delta_4 b^\mu(-\mu+\nu+n+1)a^{\frac{1}{2}(\beta+4n+\xi+2)} - \Delta_3 a^{\mu+n}b^{\frac{1}{2}(\beta+2n+\xi+2)}\big(\Delta_1\Delta_5 b^\mu(\nu+n+1) + \Delta_4(-\mu+\nu+n+1)\big) + \alpha_a(\nu+1)a^\mu(\Phi_1 b^\mu + \Phi_2)b^{\frac{1}{2}(\beta+2n+\xi+2)}\Big) \quad (34)$$

If the disk is made of an isotropic and homogeneous material, Eq. (31) turns into [42]

$$u_r''(r) + \frac{1}{r}u_r'(r) - \frac{1}{r^2}u_r(r) = (1+\nu)\alpha T'(r) = (1+\nu)\frac{\alpha}{r}\left(\frac{T_a - T_b}{\ln\left(\frac{a}{b}\right)}\right) = (1+\nu)\frac{\alpha}{r}\Psi_2 = \frac{\Delta}{r} \quad (35)$$

Solution of Eq. (35) under free-free boundary condition is

$$u_r(r) = \frac{1}{2(\nu-1)(\nu+1)r(a-b)(a+b)}\{a^2(\nu+1)lna(\Delta - 2\alpha\Psi_2)(b^2(\nu+1) - (\nu-1)r^2) - b^2(\nu+1)lnb(a^2(\nu+1) - (\nu-1)r^2)(\Delta - 2\alpha\Psi_2) + (\nu-1)r^2(a-b)(a+b)(2\alpha(\nu+1)\Psi_1 - \Delta + \Delta(\nu+1)lnr)\}$$

$$\sigma_r(r) = -\frac{E(\Delta - 2\alpha\Psi_2)(b^2(r^2-a^2)lnb + a^2 lna(b-r)(b+r) + r^2(a-b)(a+b)lnr)}{2(\nu-1)r^2(a-b)(a+b)} \quad (36)$$

$$\sigma_\theta(r) = \frac{1}{2(\nu-1)(\nu+1)r^2(a-b)(a+b)}\Big(\mathrm{E}\big((\nu+1)(\Delta - 2\alpha\Psi_2)(a^2 lna(b^2+r^2) - b^2(a^2+r^2)lnb + r^2(b^2-a^2)lnr) - \Delta(\nu-1)r^2(a-b)(a+b)\big)\Big)$$

4. Revisited the Benchmark Example

Jabbari et al. [39] and Eslami et al. [40] used the following material and geometrical properties to study the thermo-mechanical analysis of both traction-free cylinders and spheres which are subjected to both internal pressure and surface temperature differences.

$a = 1.0m; b = 1.2m; \nu = 0.3; E_a = 200\ GPa;$
$\rho_a = 7800\frac{kg}{m^3}; \alpha_a = 1.2\ 10^{-6}\frac{1}{℃};\ k_a = 15.379\frac{W}{m℃};$
$p_a = 50\ MPa;\ \ p_b = 0;\ \ T_a = 10℃;\ \ T_b = 0℃$

In the present study the same example is to be extended to a hollow disk or annulus under free-free boundary conditions. In the benchmark examples, the homogeneity indexes are to be all the same, $\beta = n = \mu = q$, and they are determined hypothetically. Jabbari et al. [39] and Eslami et al. [40] did not consider the centrifugal forces. The constant angular velocity is assumed to be $\omega = 100\ rad/s$, and the hypothetically chosen values of the inhomogeneity indexes are to be $-3 \leq \beta \leq 3$ in the present example. The results are presented in Figs. 2-3 and Table 1. It may be noted that, for the disks made of isotropic and homogeneous materials, $\beta = n = \mu = q = 0$, Eqs. (24), (30), and (36) are used in all examples instead other closed-form expressions derived for FGM discs. This allows an auto-control mechanism for the present computations.

Variations of the dimensionless elastic fields with the inhomogeneity index under individual and combined loads are illustrated in Fig. 2. Variation of the dimensionless equivalent stress with the inhomogeneity index under combined loads is also shown in Fig. 3. If the present graphs for combined thermal and pressure loads in Figs. 2-3 are compared with the benchmark graphs, it is seen that the present graphs are very close to the graphs for cylinders [39]. Fig. 2 and 3 suggest

- The rotation effects seem to be much important than the thermal effects. The thermal effects may be negligible for this example.
- As r/a increases the dimensionless radial displacement increases under individual thermal loads for all inhomogeneity indexes. Maximum combined radial displacements are observed at the inner surface.

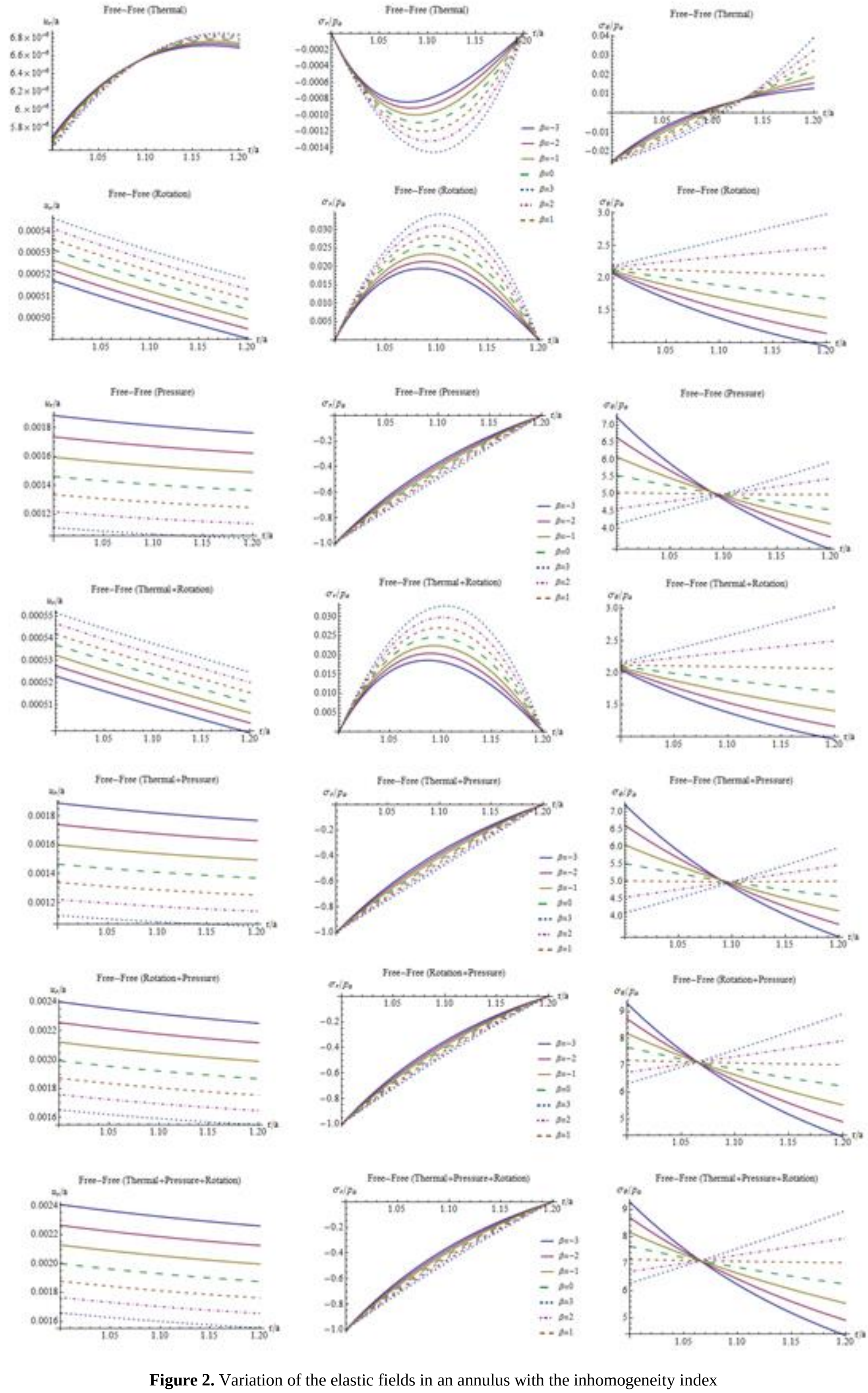

Figure 2. Variation of the elastic fields in an annulus with the inhomogeneity index

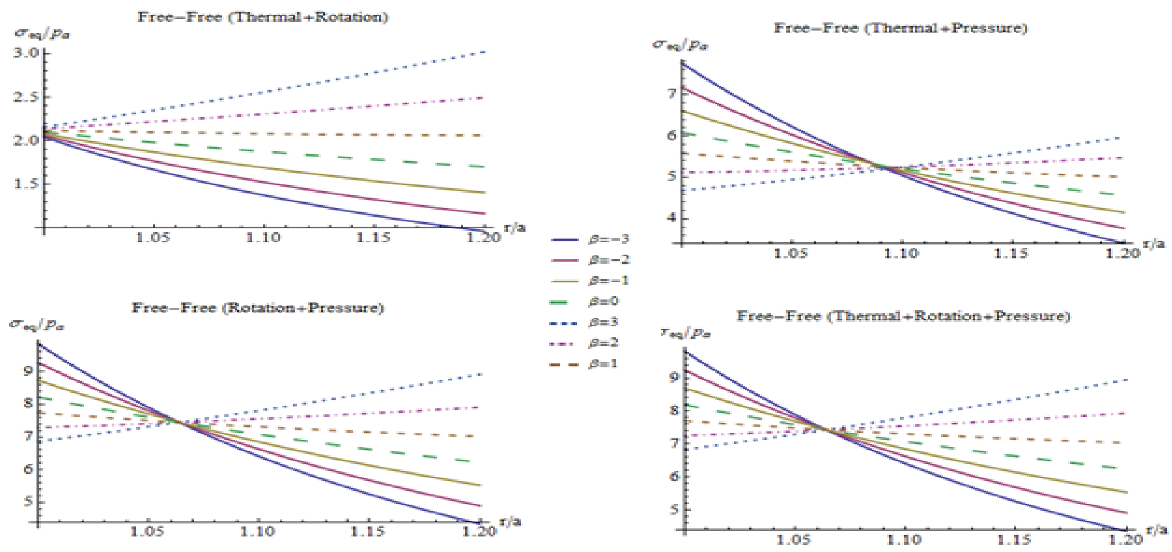

Figure 3. Variation of the dimensionless equivalent stress with the inhomogeneity index under combined loads for free-free boundary conditions.

Table 1. Variation of the dimensionless elastic fields with the inhomogeneity indexes

	u_r/a		σ_r/p_a		σ_θ/p_a	
r/a	$\beta=-2$	$\beta=2$	$\beta=-2$	$\beta=2$	$\beta=-2$	$\beta=2$
Thermal						
1.	0.00000568	0.0000056	0.	0.	-0.0252823	-0.0256429
1.04	0.00000615	0.0000061	-0.0006996	-0.0008291	-0.0117571	-0.0172315
1.08	0.00000647	0.0000065	-0.0009132	-0.0012579	-0.0016646	-0.0073190
1.12	0.00000666	0.0000067	-0.0007991	-0.0012733	0.00585425	0.00421912
1.16	0.00000674	0.0000068	-0.0004687	-0.0008510	0.011432	0.017512
1.2	0.00000671	0.0000068	0.	0.	0.0155387	0.032693
Centrifugal						
1.	0.00052199	0.0005413	0.	0.	2.08796	2.16504
1.04	0.00051597	0.0005350	0.0153977	0.0195631	1.83938	2.23156
1.08	0.00051035	0.0005292	0.0211395	0.0296796	1.62687	2.29506
1.12	0.00050504	0.0005237	0.0194235	0.0300443	1.44374	2.35514
1.16	0.00049994	0.0005184	0.0119405	0.0202913	1.28474	2.4114
1.2	0.00049496	0.0005132	0.	0.	1.14574	2.46342
Pressure						
1.	0.00173548	0.0012174	-1.	-1.	6.64192	4.56964
1.04	0.00170714	0.0011954	-0.721683	-0.782553	5.85405	4.73815
1.08	0.00168181	0.0011765	-0.490729	-0.574911	5.19307	4.90994
1.12	0.00165928	0.0011602	-0.29798	-0.375911	4.63479	5.08474
1.16	0.00163939	0.0011461	-0.136284	-0.184559	4.16027	5.26232
1.2	0.00162198	0.0011339	0.	0.	3.75458	5.4425
Combined (thermal+pressure)						
1.	0.00174116	0.001223	-1.	-1.	6.61664	4.54399
1.04	0.00171329	0.0012015	-0.722383	-0.783383	5.84229	4.72092
1.08	0.00168828	0.0011829	-0.491642	-0.576169	5.1914	4.90262
1.12	0.00166594	0.0011669	-0.29878	-0.377184	4.64064	5.08896
1.16	0.00164613	0.0011529	-0.136752	-0.185419	4.1717	5.27984
1.2	0.00162869	0.0011407	0.	0.	3.77012	5.4752
Combined (thermal+centrifugal)						
1.	0.00052767	0.0005469	0.	0.	2.06267	2.1394
1.04	0.00052212	0.0005411	0.0146981	0.018734	1.82763	2.21432
1.08	0.00051682	0.0005357	0.0202264	0.0284217	1.62521	2.28774
1.12	0.0005117	0.0005304	0.0186244	0.028771	1.44959	2.35936
1.16	0.00050668	0.0005252	0.0114718	0.0194313	1.29618	2.42891
1.2	0.00050167	0.0005200	0.	0.	1.16128	2.49612
Combined (centrifugal+pressure)						
1.	0.00225747	0.0017587	-1.	-1.	8.72988	6.73468
1.04	0.0022231	0.0017304	-0.706286	-0.76299	7.69343	6.96971
1.08	0.00219216	0.0017057	-0.469589	-0.545232	6.81994	7.20499
1.12	0.00216432	0.0016839	-0.278557	-0.345867	6.07852	7.43988
1.16	0.00213933	0.0016644	-0.124343	-0.164267	5.44502	7.67372
1.2	0.00211694	0.0016471	0.	0.	4.90032	7.90593
Combined (thermal+centrifugal+pressure)						
1.	0.00226315	0.0017643	-1.	-1.	8.7046	6.70904
1.04	0.00222925	0.0017365	-0.706985	-0.763819	7.68168	6.95248
1.08	0.00219863	0.0017121	-0.470502	-0.54649	6.81827	7.19767
1.12	0.00217098	0.0016905	-0.279356	-0.34714	6.08438	7.4441
1.16	0.00214607	0.0016713	-0.124812	-0.165127	5.45645	7.69124
1.2	0.00212365	0.0016539	0.	0.	4.91586	7.93862

- The dimensionless radial stresses are all in compression under individual thermal and pressure loads, combined (thermal+pressure), (centrifugal+pressure) and thermo-mechanical loads, viz., combined thermal, pressure and centrifugal loads. The absolute value of the maximum radial stress is observed at the vicinity of mid-surface under individual thermal, individual centrifugal, combined (thermal+centrifugal) loads while it is on the inner surface under other loads.
- Tangential stresses are all in tension except for thermal loads for all inhomogeneity indexes. Maximum hoop stress is at the inner surface for negative inhomogeneity indexes.
- While β =-1 seems to be a better choice for almost uniform equivalent stress variation under combined (thermal+centrifugal) loads, $\beta = 2$ is the best for other types of combined loads (Fig. 3).

5. Examples with Physical FGMs

In the present study, three types of physical metal-ceramic pairs are considered to understand the thermo-mechanical behavior of such structures. Material properties of the constituents are given in Table 2 for nickel-silicon nitride (Ni-Si_3N_4), aluminum-aluminum oxide (Al-Al_2O_3), and stainless steel-zirconium oxide (SUS304-ZrO_2). Contrary to the benchmark example, the inhomogeneity indexes are now to be determined exactly regarding to the types of metal and ceramic and their locations. Assume that the inner surface is to be full ceramic and the outer surface is to be full metal. In this case the intermediate surface consists of a mixture of metal and ceramic which obeys the power law gradient given by Eqs. (2) and (13). The values of inhomogeneity indexes depend on the annulus aspect ratio, *a/b*, as well as the constituents' material properties. Positive inhomogeneity index means an increase from the inner surface towards the outer. The contrary is true for negative inhomogeneity indexes. The inhomogeneity indexes are computed under this assumption as follows

$$\beta = \ln\left(\frac{E_a}{E_b}\right) / \ln\left(\frac{a}{b}\right); \quad q = \ln\left(\frac{\rho_a}{\rho_b}\right) / \ln\left(\frac{a}{b}\right);$$
$$n = \ln\left(\frac{\alpha_a}{\alpha_b}\right) / \ln\left(\frac{a}{b}\right); \quad \mu = \ln\left(\frac{k_a}{k_b}\right) / \ln\left(\frac{a}{b}\right) \tag{37}$$

Material and geometrical properties of the annulus are determined as: $\omega = 100\frac{rad}{s}$; $p_a = 30MPa$; $p_b = 5MPa$; $T_a = 373K$; $T_b = 273K$; $a = 0.5m; b = 1.0m$. Results are tabulated in Tables 3-5 and illustrated in Figs. 4-5. From those tables and figures, it is mostly observed that the thermal effects are not negligible as in the previous example since the surface temperature difference has been taken much higher than the previous example.

Combined radial displacements of three types FGMs are closer to the ceramic constituents. The radial displacements build-up as r/b increases under thermal loadings for three FGMs while they decrease with increasing r/b ratios under individual pressure and centrifugal loads. Ni/ Si_3N_4 has the smallest radial displacements than other two FGMs while Al/Al_2O_3 has the highest ones.

The characteristic variation of radial stresses of Ni/ Si_3N_4 and Al/Al_2O_3 are similar to each other to some extent. SUS304/ ZrO_2 has entirely combined thermo-mechanical radial compression stresses while the others have tension-compression in nature. It is fascinating that the behavior of FGMs are totally different from the behaviors of individual metal and ceramics under thermal loading. While individual ceramic and metal give thermal radial stresses in compression, FGM offers radial stresses in tension. Maximum combined thermo-mechanical radial stress is observed at both the inner surface and at the surface between the inner and mid-surface for both Ni/ Si_3N_4 and Al/Al_2O_3.

It is observed from Fig. 4 that the characteristic behaviors of Ni/ Si_3N_4 and Al/Al_2O_3 are similar under both individual pressure and centrifugal loads. However, Ni/ Si_3N_4 seems much proper than Al/Al_2O_3 under individual pressure while it is the worst for individual rotation. For combined thermo-mechanical loadings, SUS304/ ZrO_2 exhibits the most appropriate hoop and equivalent stresses (Figs. 4-5). The performance of SUS304/ ZrO_2 under centrifugal forces are better than the others. SUS304/ ZrO_2 also shows the best performance under individual thermal loading and combined thermal and mechanical loads.

Table 2. The physical constituent materials used in the present study

		E *(GPa)*	*ρ* *(kg/m³)*	*ν*	*k* *(W/mK)*	*α* *(1/K)*
Metal	Nickel (Ni)	199.5	8900	0.3	90.7	13.3E-6
	Aluminum (Al)	70	2700	0.3	204	23.E-6
	SUS304 (Stainless Steel)	201.04	7800	0.3262	15.379	12.33E-6
Ceramic	Silicon Nitride (Si_3N_4)	348.43	4429	0.24	1.209	5.8723E-6
	Aluminum Oxide (Al_2O_3)	393	3970	0.3	30.1	8.8E-6
	Zirconium oxide (ZrO_2)	116.4	3657	0.3	1.78	8.7E-6

Table 3. Elastic fields of circular annulus with physical FGMs (*Ni-Si_3N_4* and *Al-Al_2O_3*) under thermal and centrifugal loads

		Thermal			*Centrifugal*	
r/b	*Si_3N_4*	*Ni-Si_3N_4*	*Ni*	*Si_3N_4*	*Ni-Si_3N_4*	*Ni*
			u_r (mm)			
0.5	0.915496	1.35275	2.07348	0.0544997	0.111344	0.193781
0.6	1.13013	1.56113	2.56306	0.0527081	0.107424	0.18533
0.7	1.32442	1.79872	3.00432	0.0518973	0.106284	0.180747
0.8	1.50395	2.07772	3.41054	0.0514076	0.106298	0.177593
0.9	1.67208	2.4001	3.78969	0.0508324	0.106125	0.174377
1.	1.83099	2.76541	4.14696	0.0498919	0.10448	0.170081
			σ_r (GPa)			
0.5	0.	0.	0.	0.	0.	0.
0.6	-0.01477	0.0265844	-0.0191536	0.0035078	0.00849608	0.0071793
0.7	-0.0171497	0.0339282	-0.0222396	0.0044807	0.0108177	0.0091706
0.8	-0.0137526	0.0285571	-0.0178342	0.0039350	0.00958235	0.0080538
0.9	-0.0075515	0.0161291	-0.00979269	0.0023562	0.00583515	0.0048225
1.	0.	0.	0.	0.	0.	0.
			σ_θ (GPa)			
0.5	-0.125218	0.17949	-0.16238	0.0379787	0.0775914	0.0773188
0.6	-0.0566285	0.123614	-0.07344	0.0314503	0.0561662	0.0637759
0.7	-0.0087453	0.0326852	-0.01134	0.0269076	0.0432787	0.0542641
0.8	0.0272743	-0.0484405	0.035369	0.0233343	0.0343077	0.0467034
0.9	0.0558414	-0.116065	0.072415	0.020245	0.0271806	0.0401003
1.	0.079391	-0.172665	0.102954	0.0173838	0.0208437	0.0339313
r/b	*Al_2O_3*	*Al-Al_2O_3*	*Al*	*Al_2O_3*	*Al-Al_2O_3*	*Al*
			u_r (mm)			
0.5	1.37193	2.10962	3.58572	0.0438796	0.0680382	0.167545
0.6	1.69586	2.44523	4.43236	0.0419658	0.0652997	0.160237
0.7	1.98782	2.85505	5.19543	0.0409282	0.0645656	0.156275
0.8	2.2566	3.34168	5.89792	0.040214	0.0648825	0.153548
0.9	2.50747	3.90588	6.55361	0.0394857	0.0652246	0.150767
1.	2.74385	4.54737	7.17143	0.038513	0.0643676	0.147054
			σ_r (GPa)			
0.5	0.	0.	0.	0.	0.	0.
0.6	-0.024965	0.0363991	-0.011622	0.0032025	0.00463795	0.002178
0.7	-0.0289873	0.0364721	-0.0134946	0.0040907	0.00508015	0.0027821
0.8	-0.0232453	0.0257909	-0.0108215	0.0035925	0.00395046	0.0024433
0.9	-0.0127639	0.0126957	-0.00594201	0.0021512	0.0021415	0.001463
1.	0.	0.	0.	0.	0.	0.
			σ_θ (GPa)			
0.5	-0.211649	0.36818	-0.0985297	0.0344894	0.053478	0.0234563
0.6	-0.0957164	0.104515	-0.0445591	0.0284484	0.0285597	0.0193478
0.7	-0.0147818	-0.0160097	-0.00688143	0.0242055	0.0172121	0.0164621
0.8	0.0461005	-0.0752527	0.0214613	0.0208329	0.0110787	0.0141685
0.9	0.094386	-0.105572	0.0439398	0.0178874	0.00723665	0.0121652
1.	0.134191	-0.121214	0.0624703	0.0151356	0.00450573	0.0102938

Table 4. Elastic fields of circular annulus with physical FGMs (*Ni-Si_3N_4* and *Al-Al_2O_3*) under pressure and combined loads

	Pressures			*Thermo-mechanical*		
r/b	*Si_3N_4*	*Ni-Si_3N_4*	*Ni*	*Si_3N_4*	*Ni-Si_3N_4*	*Ni*
			u_r (mm)			
0.5	0.062949	0.079638	0.114453	1.03294	1.54374	2.38171
0.6	0.053791	0.069195	0.097522	1.23663	1.73775	2.84591
0.7	0.047456	0.061447	0.085762	1.42377	1.96645	3.27082
0.8	0.042888	0.055445	0.077235	1.59824	2.23946	3.66537
0.9	0.039496	0.050644	0.070862	1.76241	2.55687	4.03493
1.	0.036928	0.046708	0.065998	1.91781	2.9166	4.38304
			σ_r (GPa)			
0.5	-0.03	-0.03	-0.03	-0.03	-0.03	-0.03
0.6	-0.0198148	-0.0187403	-0.0198148	-0.031077	0.016340	-0.031789
0.7	-0.0136735	-0.0125855	-0.0136735	-0.0263425	0.032160	-0.026743
0.8	-0.0096875	-0.0089115	-0.0096875	-0.019505	0.029228	-0.019468
0.9	-0.0069547	-0.0065699	-0.0069547	-0.01215	0.015394	-0.011925
1.	-0.005	-0.005	-0.005	-0.005	-0.005	-0.005
			σ_θ (GPa)			
0.5	0.0366667	0.0473966	0.0366667	-0.05057	0.304478	-0.048396
0.6	0.0264815	0.0296411	0.0264815	0.001303	0.209421	0.016822
0.7	0.0203401	0.0199344	0.0203401	0.038502	0.0958984	0.0632634
0.8	0.0163542	0.0141393	0.0163542	0.066963	$6.543.10^{-6}$	0.0984268
0.9	0.0136214	0.0104453	0.0136214	0.089708	-0.0784388	0.126136
1.	0.0116667	0.0079682	0.0116667	0.108442	-0.143853	0.148552
r/b	*Al_2O_3*	*Al-Al_2O_3*	*Al*	*Al_2O_3*	*Al-Al_2O_3*	*Al*
			u_r (mm)			
0.5	0.0581001	0.106582	0.32619	1.47391	2.28424	4.07945
0.6	0.0495052	0.0946808	0.277937	1.78733	2.60521	4.87054
0.7	0.0435357	0.0847664	0.244422	2.07228	3.00439	5.59613
0.8	0.039207	0.07593	0.220119	2.33602	3.48249	6.27159
0.9	0.0359721	0.0675964	0.201958	2.58292	4.0387	6.90633
1.	0.033503	0.0593678	0.188095	2.81587	4.6711	7.50658
			σ_r (GPa)			
0.5	-0.03	-0.03	-0.03	-0.03	-0.03	-0.03
0.6	-0.0198148	-0.0164097	-0.0198148	-0.0415773	0.024627	-0.029259
0.7	-0.0136735	-0.0105156	-0.0136735	-0.0385701	0.031037	-0.024386
0.8	-0.0096875	-0.0075873	-0.0096875	-0.0293403	0.022154	-0.018066
0.9	-0.0069547	-0.0059712	-0.0069547	-0.0175675	0.008866	-0.011434
1.	-0.005	-0.005	-0.005	-0.005	-0.005	-0.005
			σ_θ (GPa)			
0.5	0.0366667	0.0747737	0.0366667	-0.140493	0.496432	-0.038407
0.6	0.0264815	0.0344695	0.0264815	-0.0407865	0.167544	0.0012701
0.7	0.0203401	0.0174417	0.0203401	0.0297638	0.018644	0.0299209
0.8	0.0163542	0.009302	0.0163542	0.0832876	-0.05487	0.051984
0.9	0.0136214	0.0050426	0.0136214	0.125895	-0.09329	0.0697264
1.	0.0116667	0.0026557	0.0116667	0.160993	-0.11405	0.0844307

Table 5. Elastic fields of circular annulus with $SUS304 - ZrO_2$.

	Thermal			*Centrifugal*		
r/b	ZrO_2	$SUS304 - ZrO_2$	$SUS304$	ZrO_2	$SUS304 - ZrO_2$	$SUS304$
			$u_r\ (mm)$			
0.5	1.35634	1.5991	1.92226	0.13647	0.173756	0.169483
0.6	1.67659	1.91271	2.37753	0.130518	0.165861	0.161298
0.7	1.96523	2.21899	2.7871	0.127291	0.161489	0.156647
0.8	2.23095	2.53105	3.16354	0.125069	0.158363	0.153359
0.9	2.47897	2.8539	3.51438	0.122804	0.155188	0.150113
1.	2.71267	3.18944	3.84451	0.119779	0.151119	0.146012
			$\sigma_r\ (GPa)$			
0.5	0.	0.	0.	0.	0.	0.
0.6	-0.00731	0.001025	-0.01789	0.002950	0.004511	0.0063420
0.7	-0.00849	0.002963	-0.02078	0.003768	0.006304	0.0081010
0.8	-0.00681	0.003702	-0.01666	0.003309	0.006010	0.0071144
0.9	-0.00374	0.002721	-0.00915	0.001982	0.003883	0.00426
1.	0.	0.	0.	0.	0.	0.
			$\sigma_\theta\ (GPa)$			
0.5	-0.06197	-0.00546	-0.1517	0.031770	0.040451	0.0681457
0.6	-0.02803	0.013470	-0.06861	0.026206	0.038564	0.0561143
0.7	-0.00433	0.013459	-0.01059	0.022297	0.036985	0.0476314
0.8	0.013499	0.002947	0.03304	0.019190	0.035259	0.0408597
0.9	0.027638	-0.01408	0.06765	0.016477	0.033118	0.0349215
1.	0.039293	-0.03551	0.096182	0.013942	0.030381	0.0293543
		Pressures			*Thermo-mechanical*	
			$u_r\ (mm)$			
0.5	0.196163	0.157868	0.115531	1.68897	1.93073	2.20727
0.6	0.167144	0.131506	0.098324	1.97425	2.21007	2.63715
0.7	0.146989	0.114426	0.086352	2.23951	2.49491	3.0301
0.8	0.132374	0.102797	0.077653	2.4884	2.79221	3.39455
0.9	0.121452	0.094606	0.071135	2.72323	3.10369	3.73562
1.	0.113116	0.088701	0.066144	2.94557	3.42926	4.05667
			$\sigma_r\ (GPa)$			
0.5	-0.03	-0.03	-0.03	-0.03	-0.03	-0.03
0.6	-0.01981	-0.02084	-0.01981	-0.02418	-0.01530	-0.0313666
0.7	-0.01367	-0.01480	-0.01367	-0.01839	-0.00553	-0.0263493
0.8	-0.00969	-0.01055	-0.00969	-0.01318	-0.00084	-0.0192342
0.9	-0.00695	-0.00741	-0.00695	-0.00871	-0.00080	-0.0118433
1.	-0.005	-0.005	-0.005	-0.005	-0.005	-0.005
			$\sigma_\theta\ (GPa)$			
0.5	0.036667	0.027359	0.036667	0.006462	0.062351	-0.0468881
0.6	0.026482	0.022931	0.026482	0.024660	0.074965	0.0139907
0.7	0.020340	0.020174	0.020340	0.038309	0.070618	0.0573767
0.8	0.016354	0.018363	0.016354	0.049044	0.056569	0.0902567
0.9	0.013621	0.017129	0.013621	0.057736	0.036171	0.116194
1.	0.011667	0.016267	0.011667	0.064902	0.011134	0.137203

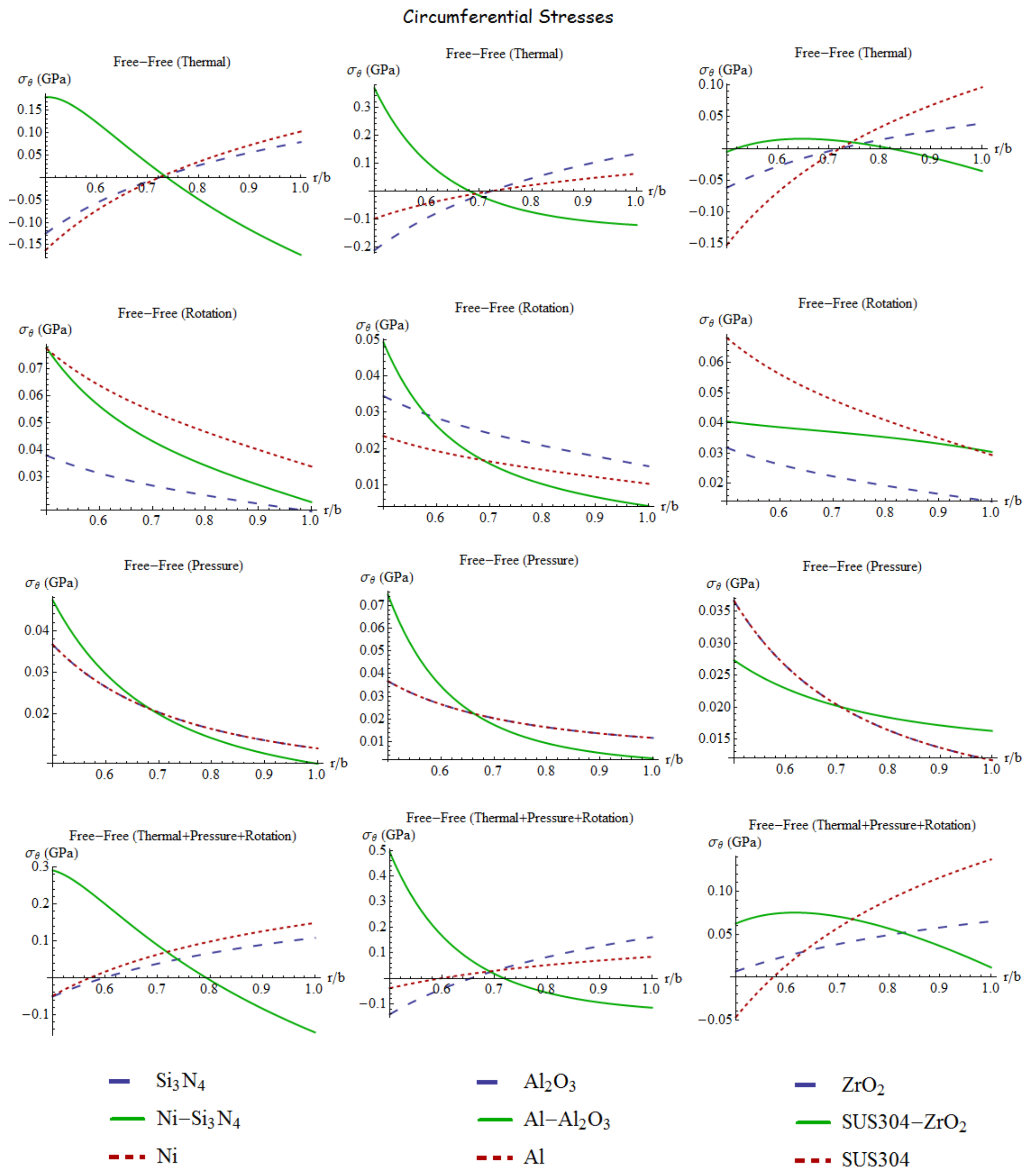

Figure 4. Variation of the hoop stress with FGM types under individual and combined loads

6. Conclusions

The present study addresses exact thermo-mechanical analysis of a rotating FGM circular annulus or disc. After proposing closed form solutions for separate loads such as centrifugal, thermal, and pressure, two parametric studies are conducted. The first study is related to the benchmark example with hypothetically chosen inhomogeneity parameters. This example is originally handled for circular annuli in this manuscript. The second study considers the thermo-mechanical behavior of three types of physical ceramics, metals, and FGMs.

Separate and combined effects of each loading are studied in two examples. Those studies generally imply that the effect of thermal loads may be either negligible compared to inertia forces as in the first benchmark example or may be having higher importance than the inertias as in the second example. It is also concluded that the thermal characteristics of both individual metal and ceramic are totally different from FGM's thermal traits. The author hopes that both the formulas proposed in the present study and graphs are to be helpful for the demands of the related industries.

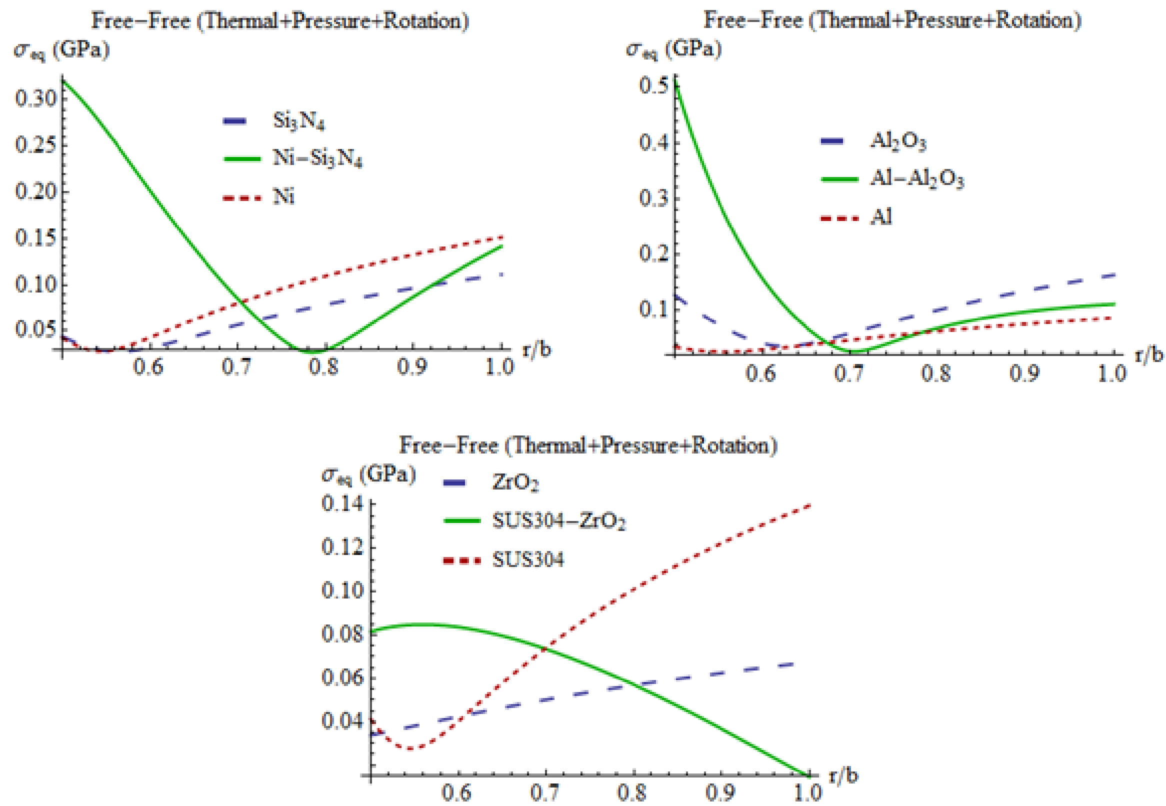

Figure 5. Variation of the equivalent stress with FGMs under combined loads

References

[1] B.S. Reddy, J. S. Kumar, C.E. Reddy, K.V.K. Reddy, “Static Bending Behavior of Functionally Graded Plates Subjected to Mechanical Loading”. Jordan Journal of Mechanical and Industrial Engineering, JJMIE, Vol. 8, No. 4, 2014, 193-206.

[2] H. Eskandari, “Three-dimensional investigations of stress intensity factors in a rotating thick-walled FGM cylinder”. Jordan Journal of Mechanical and Industrial Engineering, JJMIE, Vol. 10, No. 2, 2016, 105-113.

[3] C.O. Horgan, A.M. Chan, “The stress response of functionally graded isotropic linearly elastic rotating disks”. Journal of Elasticity, Vol. 55, No. 3, 1999, 219-230.

[4] J.F. Durodola, O. Attia, “Deformation and stresses in FG rotating disks”. Compos Sci Technol, Vol. 60, 2000, 987–995.

[5] A.M. Zenkour, “Analytical solutions for rotating exponentially-graded annular disks with various boundary conditions”. Int J Str Stab Dyn, Vol. 5, No. 4, 2005, 557-577.

[6] A.M. Zenkour, “Elastic deformation of the rotating functionally graded annular disk with rigid casing”. J Mater Sci, Vol. 42, 2007, 9717–9724.

[7] A.N. Eraslan, T. Akiş, “On the plane strain and plane stress solutions of functionally graded rotating solid shaft and solid disk problems”. Acta Mechanica, Vol. 181, No. 1–2, 2006, 43–63.

[8] M. Asghari, E. Ghafoori, “A three-dimensional elasticity solution for functionally graded rotating disks”. Composite Structures, Vol. 92, No. 5, 2010, 1092-1099.

[9] H. Argeso, “Analytical solutions to variable thickness and variable material property rotating disks for a new three-parameter variation function”. Mech Based Des Struc, Vol. 40, No. 2, 2012, 133-152.

[10] X.L. Peng, X.F. Li, “Effects of gradient on stress distribution in rotating functionally graded solid disks”. J Mech Sci Technol, Vol. 26, 2012, 1483-1492.

[11] M.Z. Nejad, A. Rastgoo, A. Hadi, “Exact elasto-plastic analysis of rotating disks made of functionally graded materials”. Int J Eng Sci, Vol. 85, 2014, 47-57.

[12] T. Dai, H.L. Dai, “Investigation of mechanical behavior for a rotating FGM circular disk with a variable angular speed”. J Mech Sci Technol, Vol. 29, No. 9, 2015, 3779-3787.

[13] H. Çallıoğlu, M. Sayer, E. Demir, “Elastic–plastic stress analysis of rotating functionally graded discs”. Thin-Walled Structures, Vol. 94, 2015, 38-44.

[14] C.O. Horgan, A.M. Chan, “The pressurized hollow cylinder or disk problem for functionally graded isotropic linearly elastic materials”. Journal of Elasticity, Vol. 55, No. 1, 1999, 43-59.

[15] L.H. You, J.X. Wang, B.P. Tang, “Deformations and stresses in annular disks made of functionally graded materials subjected to internal and/or external pressure”. Meccanica, Vol. 44, 2009, 283-292.

[16] N. Tutuncu, B. Temel, “A novel approach to stress analysis of pressurized FGM cylinders, disks and spheres”. Composite Structures, Vol. 91, 2009, 385-390.

[17] M.H. Lotfian, M.Z. Nejad, M. Abedi, M. Ghannad, “An elasticity solution for functionally graded hollow disks under radially symmetry loads”. J Basic Appl Sci Res, Vol. 1, No. 11, 2011, 2435-2441.

[18] M.Z. Nejad, M. Abedi, M.H. Lotfian, M. Ghannad, “Elastic analysis of exponential FGM disks subjected to internal and external pressure”. Central European Journal of Engineering, Vol. 3, No. 3, 2013, 459-465.

[19] N. Noda, “Thermal stress in materials with temperature-dependent properties”. Appl Mech Rev, Vol. 44, No. 9, 1991, 383–397.

[20] Y. Tanigawa, "Some basic thermoplastic problems for nonhomogeneous structural materials". Appl Mech Rev, Vol. 48, 1995, 377–389.

[21] M. Bakshi, A. Bagri, M.R. Eslami, "Coupled thermoelasticity of functionally graded disk". Mech Adv Mater Struct, Vol. 13, 2006, 219–225.

[22] Y.V. Tokovy, C.C. Ma, "Thermal stresses in anisotropic and radially inhomogeneous annular domains". J. Therm. Stress, Vol. 31, 2008, 892–913.

[23] A.M. Zenkour, "Thermoelastic analysis of an annular sandwich disk with metal/ceramic faces and functionally graded core". J Thermoplas Compos, Vol. 22, 2009, 163–181.

[24] X.L. Peng, X.F. Li, "Thermoelastic analysis of functionally graded annulus with arbitrary gradient". Appl. Math. Mech. -Engl. Ed., Vol. 30, No. 10, 2009, 1211–1220.

[25] B. Arnab, S.M.R. Islam, A.A. Khalak, A.M. Afsar, "Finite difference solution to thermoelastic field in a thin circular FGM disk with a concentric hole". Procedia Engineering, Vol. 90, 2014, 193-198.

[26] N.N. Aleksandrova, "Effect of thermal gradients on stress/strain distributions in a thin circular symmetric plate". Structural Engineering and Mechanics, Vol. 58, No. 4, 2016, 627-639.

[27] H. Çallıoğlu, M. Sayer, E. Demir, "Stress analysis of functionally graded discs under mechanical and thermal loads". Indian J Eng Mater Sci, Vol. 18, 2011, 111-118.

[28] A.Kursun, M. Topçu, T. Tetik, "Stress analysis of functionally graded disc under thermal and mechanical loads". Procedia Engineering, Vol. 10, 2011, 2949–2954.

[29] D. Gönczi, I. Ecsedi, "Thermoelastic analysis of functionally graded hollow circular disc". Archive of Mechanical Engineering, Vol. LXII, No. 1, 2015, 5-18.

[30] A.M. Zenkour, "On the magneto-thermo-elastic responses of FG annular sandwich disks", International Journal of Engineering Science, Vol. 75, 2014, 54–66.

[31] A.M. Zenkour, "Steady-state thermoelastic analysis of a functionally-graded rotating annular disk". International Journal of Structural Stability and Dynamics, Vol. 6, No. 4, 2006, 1-16.

[32] S.A.H. Kordkheili, R. Naghdabadi, "Thermoelastic analysis of a functionally graded rotating disk". Compos Struct, Vol. 79, No. 4, 2007, 508–516.

[33] J. Go, A.M. Afsar, J.I. Song, "Analysis of thermoelastic characteristics of a rotating FGM circular disk by finite element method". Adv Compos Mater, Vol. 19, No. 2, 2010, 197–213.

[34] A.M. Afsar, J. Go, J.I. Song, "A mathematical analysis of thermoelastic characteristics of a rotating circular disk with an FGM coating at the outer surface". Adv Compos Mater, Vol. 19, No. 3, 2010, 269-288.

[35] A.M. Afsar, J. Go, "Finite element analysis of thermoelastic field in a rotating FGM circular disk". Applied Mathematical Modelling, Vol. 34, 2010, 3309-3320.

[36] A.M. Afsar, F.A. Sohag, "Effect of FGM coating on thermoelastic characteristics of a rotating circular disk". Proceedings of MARTEC 2010, The International Conference on Marine Technology, 11-12 December BUET, Dhaka, Bangladesh. 2010, 459-464.

[37] J.F. Gong, P.J. Ming, L.K. Xuan, W.P. Zhang, "Thermoelastic analysis of three dimensional functionally graded rotating disks based on finite volume method". Proc. Inst. Mech. Eng. C: Journal of Mechanical Engineering Science. Vol. 228, No. 4, 2014, 583-598.

[38] V. Yıldırım, "Thermomechanical characteristics of a functionally graded mounted uniform disc with/without rigid casing". The Journal of Aerospace Technology and Management (JATM), Vol. 11, 2019, http://dx.doi.org/10.5028/jatm.v11.1008

[39] M. Jabbari, S. Sohrabpour, M.R. Eslami, "Mechanical and thermal stresses in a functionally graded hollow cylinder due to radially symmetric loads". Int J Pressure Vessels and Piping, Vol. 79, 2002, 493–497.

[40] M.R. Eslami, M.H. Babaei, R. Poultangari, "Thermal and mechanical stresses in a functionally graded thick sphere". Int J Pressure Vessel Piping. Vol. 82, 2005, 522–527.

[41] V. Yıldırım, "Exact thermal analysis of functionally graded cylindrical and spherical vessels". International Journal of Engineering & Applied Sciences (IJEAS), Vol. 9, No. 2, 2017, 112-126. doi.org/10.24107/ijeas.318459

[42] V. Yıldırım, "Heat-induced, pressure-induced and centrifugal-force-induced exact axisymmetric thermo-mechanical analyses in a thick-walled spherical vessel, an infinite cylindrical vessel, and a uniform disk made of an isotropic and homogeneous material". International Journal of Engineering & Applied Sciences (IJEAS), Vol. 9, No. 2, 2017, 66-87. http://dx.doi.org/10.24107/ijeas.309786

[43] V. Yıldırım, "Analytic solutions to power-law graded hyperbolic rotating discs subjected to different boundary conditions**".** International Journal of Engineering & Applied Sciences (IJEAS), Vol. 8, No. 1, 2016, 38-52.